NEXT LEVEL QUANTUM INFORMATION PROCESSING FOR SCIENCE AND TECHNOLOGY

DELIVERABLE D2.1 – REPORT ON QUANTUM SIMULATION OF CHIRAL SYMMETRY BREAKING AND FRACTIONAL EXCITATION PATTERNS IN MULTIFLAVOR ABELIAN GAUGE THEORIES

Grant Agreement:	101080086
Project Title:	NEXT LEVEL QUANTUM INFORMATION PROCESSING FOR SCIENCE AND TECHNOLOGY
Project Acronym:	NeQST
Project Start Date:	01 November 2022
Deliverable Number and title:	D2.1 - REPORT ON QUANTUM SIMULATION OF CHIRAL SYMMETRY BREAKING AND FRACTIONAL EXCITATION PATTERNS IN MULTIFLAVOR ABELIAN GAUGE THEORIES
Related Work Package:	WP2 – Quantum simulation algorithms for Abelian and non-Abelian gauge theories
Due Date:	30 April 2024
Submission date:	30 April 2024
Type:	R
Dissemination Level:	Public

Funded by the European Union

Funded by the European Union. Views and opinions expressed are however those of the author(s) only and do not necessarily reflect those of the European Union or the European Commission. Neither the European Union nor the granting authority can be held responsible for them.

Authors

	Name	Beneficiary
Lead Editor	Philipp Hauke	UNITN
Contributors	Maciej Lewenstein	ICFO
	Matteo Michele Wauters	UNITN
	Martin Ringbauer	UIBK
	Sebastian Schmitt	HRI-EU
	Daniel Müssig	Fraunhofer IOSB-AST
Revisors	Pavel Popov, Paolo Stornati	ICFO

History of change

Version	Date	Contributor	Additional information
0.1	05/02/2024	Philipp Hauke (UNITN), Maciej Lewenstein (ICFO)	Outline and preliminary draft
1.0	10/04/2024	Philipp Hauke (UNITN)	First version
1.1	12/04/2024	Pavel Popov, Paolo Stornati (ICFO)	Revisions and integration of technical information
1.2	15/04/2024	Matteo Michele Wauters (UNITN)	Quality check
2.0	17/04/2024	Philipp Hauke (UNITN)	Second version
2.1	23/04/2024	Martin Ringbauer (UIBK), Sebastian Schmitt (HRI-EU), Daniel Müssig (Fraunhofer IOSB-AST)	Minor revisions, quality check
3.0	24/04/2024	Philipp Hauke (UNITN)	Finalisation of the document

Executive Summary

This report outlines the developments within NeQST towards quantum simulation of chiral symmetry breaking and fractional excitation patterns in multiflavor abelian gauge theories.

While quantum simulation of gauge theories has made fast progress over the recent years, almost all implementations consider a single flavor of matter. It is a crucial next step of quantum simulation to move beyond this paradigm: Theories that describe nature often are naturally described by multiple flavors, such as isospin; multiflavor theories provide a natural stepping stone to non-Abelian theories with colour charge; and they can pose severe sign problems, and thus represent stringent test beds for quantum simulators. To make multiflavor theories amenable to quantum simulation, we have chosen a particularly relevant one, quantum electrodynamics on a ring. In the semiclassical regime in the continuum, it has been shown that this theory, the so-called multi-flavor Schwinger model, hosts gauge field configurations with fractional topological charge, so-called fractons. To date, it is, however, not clear how these persist in the strongly coupled regime and in particular on a lattice, the natural regimes of application of quantum simulators.

With the input of UIBK, ICFO and UNITN, have developed an implementation of the multi-flavor Schwinger model for the trapped-ion qudits platform that is being developed within NeQST. The approach is based on a variational algorithm that is implementable with abilities already demonstrated in the laboratory. Further, we have identified smoking gun observables to demonstrate the presence of fractional gauge field configurations, which is particularly challenging as the vector potential used in previous works is not accessible in the non-perturbative many-body regime we are interested in. We have performed detailed numerical benchmarks, which connects to other certification approaches developed by ICFO and CFT-PAS and which will be relevant input for the simulator suite developed by TUM. Thanks to these simulations, we have identified the scaling of resources and the minimal requirements to observe the fractional configurations, finding an excellent match to the resources already available in the qudit platform. In parallel, UIBK has demonstrated an experimental demonstration of an Abelian lattice gauge theory in 2+1 dimensions. Together, these results present a blueprint for the measurement of fracton excitations in qudit quantum simulators.

Contents

1 Introduction

The report corresponds to the deliverable *"D2.1 Report on quantum simulation of chiral symmetry breaking and fractional excitation patterns in multiflavor Abelian gauge theories"*. It summarizes the work of work package *"WP2 Quantum simulation algorithms for Abelian and non-Abelian gauge theories"* within *"Task 2.1"* until project month 18.

In this WP, mainly the University of Trento (UNITN), ICFO–The Institute of Photonic Sciences (ICFO), University of Innsbruck (UIBK), and the Technical Universiy of Munich (TUM) work together to develop protocols for quantum simulation of lattice gauge theories. In particular, UNITN and ICFO develop the theoretical frameworks, including the identification of relevant observables and field-theoretic interpretations, and perform numerical benchmarks, UIBK provides expertise on hardware requirements and performs experimental implementations, and TUM develops a software framework for the efficient simulations and representations of quantum states. Relevant synergies occur with WP1 on quantum hardware and software control, with HRI-EU and Fraunhofer IOSB-AST on algorithm design (WP3), and with CFT and ICFO on certification on quantum devices and algorithms (WP4).

The rest of this Deliverable reports on our results on quantum simulations of chiral symmetry breaking and fractional excitation patterns in multi-flavor Abelian gauge theories. In this introduction, we discuss the importance of the problem and present the state of the art, focusing on two aspects of quantum simulations (QSs) of Lattice Gauge Theories (LGTs): the use of qudits as well as multi-flavor theories as targets. The scientific results are presented in Sec. 2, and we draw our conclusions in Sec. 3 and put them into further context. Certain technical details are delegated to Appendices.

1.1 Importance of the problem

The simulation of LGTs plays a fundamental role in the theoretical understanding of fundamental interactions. Even though from the beginning of Monte Carlo simulations [1] there have been major successes in the numerical study of quantum chromodynamics (QCD) and other field theories on the lattice [2, 3], there are still open questions that cannot be addressed with this standard method. The infamous sign problem prevents the study of QCD at finite baryon density and thus makes first-principles simulations of exotic natural objects like neutron stars infeasible [2]. Quantum simulation emerges as a main candidate to overcome these challenges, promising a new era where quantum systems are harnessed to study complex quantum phenomena directly [4]. Quantum simulators are naturally sign-problem-free and can tackle long-standing fundamental questions in high-energy and condensed matter physics. Among the plethora of models that can be explored, (1+1)-dimensional quantum electrodynamics, famously known as the Schwinger Model, offers a fertile testing ground. This model captures the essence of quantum field theories, such as QCD, in a simpler, more manageable form, and has thus facilitated insights into phenomena like charge confinement, topological theta vacua, and chiral symmetry breaking. Understanding the subtle mechanisms behind these phenomena is fundamental for theoretical physics, particularly when exploring gauge field theories and supersymmetric models. For example, investigations into Euclidean path integrals reveal the importance of sectors with non-zero topological charge. While initially only integer topological sectors have been considered, configurations with fractional topological charge are vital in resolving paradoxes related to non-vanishing gluino condensates in supersymmetric Yang–Mills theory, which cannot be directly achieved through traditional methods that consider only integer topological charges. Similarly, in non-Abelian gauge theories fractional topological configurations can explain the mechanisms behind fermion condensate formation where standard approaches fall short. However, almost all of these insights derive from semi-classical arguments, and it is not certain if and how they persist in strongly-coupled theories.

In this work, we discuss the presence of these configurations in the full non-perturbative quantum many-body regime of a paradigmatic gauge theory. To achieve this with manageable resources, our study dives into the Schwinger model of quantum electrodynamics (QED) with two fermionic flavours on a circle. In our study, we employ both periodic and flavor-dependent twisted boundary conditions. These have an essential influence on the symmetry properties of the theory and thus allow for the exploration of a fractional chiral condensate in the ground state. This phenomenon is connected to the appearance of fracton gauge-field configurations, which were studied in previous analytical work with semi-classical approximations [5]. The persistence of these fractional excitations is not guaranteed in the passage from the perturbative to the non-perturbative regime. To perform efficient classical tensor network simulation, we employ a cutoff of the local Hilbert space of the gauge fields in the range $S = 1, 2, 3$. Even in this strong truncation regime, we observe the persistence of fracton excitations at finite volume, and we can even quantitatively confirm the perturbative continuum predictions. These results demonstrate the importance of fractional gauge-field configurations in strongly coupled lattice models.

The ability to explore these fractons in truncated lattice theories opens the door to studying them in existing quantum hardware. In fact, the Schwinger model with $N \geq 3$ flavors develops a strong sign problem, preventing powerful Monte-Carlo methods, making them a relevant target for the naturally sign-problem-free quantum simulators. Leveraging these novel possibilities, we discuss the necessary resources for quantum simulating fractons, demonstrating the feasibility in state-of-the-art trapped-ion qudit quantum devices, as are available within the NeQST project.

In a broader perspective, this work significantly widens the possibilities and scenarios amenable to quantum simulation. In particular, multi-flavour gauge theories are important if one aims to model the isospin. Also, the multiple flavours require a non-trivial increase of the degrees of freedom that need to be controlled, without however the full problematics of handling multiple colour charges with the associated non-Abelian symmetry. Thus, multiflavor theories represent a crucial intermediate step toward the quest for non-Abelian theories.

1.2 State of the art

While much progress has been achieved in recent years in quantum simulation of LGTs, the large potential of using qudits has been realized only recently, triggered also by significant experimental progress. Moreover, multiflavor theories have been considered only in very few proposals. In what follows, we briefly review the state of the art of both aspects.

1.2.1 Quantum simulators of Lattice Gauge Theories with qudits

The NeQST consortium was among the pioneers of gauge-theory quantum simulators with qudits, including significant individual and joint contributions before the start of the NeQST project. Important contributions include proposals and implementations for Abelian and non-Abelian LGTs using long spins, first focusing on cold atomic gases. Initial collaborations of UniTN and ICFO with theory and experimental groups in Heidelberg on gauge-theories [6–9], were extended later also to universal atomic qudit-based schemes for cold-atom quantum computers [10] including practical applications [11]. The use of qudits for LGT implementations using qudit systems is only recently gaining attention, for example [12, 13].

1.2.2 Quantum simulators of multi-flavor gauge theories

To date, almost no proposals exist to implement multi-flavour gauge theories in quantum simulators. A notable exception is Ref. [14], where it was proposed to use a digital quantum computer to simulate the $N = 3$ Schwinger model, which suffers from a severe sign problem.

In the context of classical simulation techniques using tensor networks, which traditionally have generated strong synergies with quantum simulation, the multi-flavor Schwinger model has attracted some attention since about 10 years ago, e.g., [15].

2 Fractons in the multi-flavor Schwinger model

This main section of the report presents our results on quantum simulating fractionalized gauge-field configurations of the multi-flavor Schwinger model using trapped-ion qudit hardware.

In what follows, we will first give a brief overview of the physical properties of the Schwinger Model in the continuum model and discuss how the fractional condensation of the fermions in the systems arises from the presence of twisted boundary conditions. We then introduce the lattice realization of the model used for the numerics based on exact diagonalization and tensor-network techniques. The most important results constitute the identification of signatures of fractionalized gauge configurations that become visible in lattice models amenable for qudit quantum simulation. We conclude by describing a quantum-simulation protocol based on a variational algorithm.

2.1 Fractional gauge configurations in path-integral formulations of the multi-flavor Schwinger model

We consider (1+1)-dimensional QED with N fermionic flavours, living on a cylinder $\mathbb{R} \times S$ that is closed in the spatial direction. We denote its circumference as L and its volume as $V = \mathbb{R} \times L$. The action of the theory is

$$S = \int_V d^2x \Big\{ -\frac{1}{4} F_{\mu\nu}^2 + i \sum_{p=1}^{N} \bar{\psi}_p \not{D} \psi_p - \sum_{p=1}^{N} m_p \bar{\psi}_p \psi_p \Big\} , \tag{1}$$

where $D_\mu = \partial_\mu - ieA_\mu$ is the covariant derivative, capturing the gauge-field–matter interactions.

When flavour-independent ("standard") boundary conditions are imposed on the fermions, i.e., $\psi_p(x+L) = e^{i\alpha}\psi_p(x)\ \forall p \in \{1, \cdots, N\}$, potentially with a flavour-independent phase α, the system has a $SU(N)_L \otimes SU(N)_R$ flavour symmetry in the zero mass limit, prohibiting the generation of a chiral condensate due to the Coleman theorem [16]. However, in case the boundary conditions become flavour dependent, i.e., the phase α becomes a function of the flavour index, e.g., $\alpha_p = 2\pi p/N$, the chiral symmetry is explicitly broken and chiral condensation is allowed even for vanishing rest masses.

Indeed, for small volumes ($eL \ll 1$), semi-classical arguments [5] suggest a non-vanishing chiral condensate in the presence of flavour-dependent boundary conditions. The main ingredient of this analysis is a new symmetry, induced by the transformation

$$\begin{aligned} &A_1(x) \to A_1(x) + \frac{2\pi}{NeL}, \\ &\psi_p(x) \to \psi_{p+1}(x) \text{ for } p \in \{1, \cdots, N-1\}, \\ &\psi_N(x) \to e^{-i2\pi x/L}\psi_1(x) . \end{aligned} \tag{2}$$

This combination of broken chiral symmetry and forbidden gauge transformation is absent for standard boundary conditions but emerges as a new symmetry for flavour-twisted boundary conditions. It requires one to impose a new superselection rule, one in which the noncontractable circle in the space of gauge fields is reduced by the number of flavours N.

Obtaining the same result beyond the small volume approximation is quite subtle. Within the semi-classical path-integral machinery, the chiral condensate can be calculated through the partition function $Z(m)$ as a function of the fermion mass m as

$$\langle \bar{\psi}\psi \rangle = -\frac{\partial}{\partial m} \ln Z(m)|_{m=0}. \tag{3}$$

At small mass, the partition function can be approximated as $Z(m) \propto m^{|\nu_2|N}$, where

ν_2 is the two-dimensional equivalent of the Pontryagin class

$$\nu_2 = \frac{e}{4\pi} \int_V d^2x \epsilon_{\mu\nu} F_{\mu\nu} \,. \tag{4}$$

Invoking, as is usual, the index theorem to constrain ν_2 to integer values, Eq. (3) predicts that for $N > 1$ no chiral condensate can be generated, in contradiction to the small-volume arguments. This apparent paradox can be resolved if we assume that there is a sector in the gauge field configurations with a fractional topological charge $\nu_2 = 1/N$ that contributes to the chiral condensation, as can be seen directly by inserting $Z(m) \propto m$ into Eq. (3). Turning things around, finding a non-vanishing chiral condensate in the presence of the symmetry given by Eq. (2) implies the existence of gauge field configurations with a fractional winding, so-called fractons. We will use this further below as a smoking gun in our computations on strongly-coupled lattice models.

By including fractons in the path integral, the results become consistent with the semi-classical analysis for small volumes and one obtains predictions for the full L-dependent chiral condensate [5],

$$\langle \bar{\psi}\psi \rangle = \sqrt{\frac{\mu e^{\gamma}}{16\pi L}} e^{-I/2}, \tag{5}$$

where

$$I = \int_0^\infty \frac{d\omega}{\sqrt{\omega^2 + \mu^2}} \left(\coth \frac{L\sqrt{\omega^2 + \mu^2}}{2} - 1 \right), \tag{6}$$

with the photon mass $\mu^2 = Ne^2/\pi$ and γ the Euler's constant.

However, to date it is not clear whether the fractons persist once quantum fluctuations become relevant. The above analysis holds strictly speaking for the continuum Schwinger model. It is not a priori obvious that a strongly interacting many-body lattice version of this model will exhibit qualitatively and quantitatively the same physics. As one difficulty, such many-body versions of the Schwinger model usually require finite truncation on the gauge field-Hilbert space, which makes it impossible to define a vector potential, in analogy to the difficulty in defining a phase operator. This fact obstructs the usual semi-classical argumentation for fractional windings, which are essential in demonstrating the existence of fractons.

In this report, we present our efforts leading to answering precisely this question—can we find a signature for fracton contribution to the ground state physics of a many-body system, and in particular one that can be implemented in present days quantum hardware?

2.2 Truncated lattice Schwinger model

One way to make the continuum theory suitable for the simulation techniques developed for many-body systems is to formulate a lattice many-body Hamiltonian for the gauge theory. The seminal work of Kogut and Susskind [17], now used as a standard in the context of lattice gauge theories formulations, gives a prescription how to put the degrees of freedom of the continuum gauge theory on a lattice. Thereby, the central property of the theory—the local or gauge symmetry, takes the form of local constraints between the matter and the gauge field degrees of freedom. The lattice Hamiltonian commutes with these constraints on each lattice site and therefore only gauge invariant terms are allowed—the typical correlated hopping of matter with corresponding change of the gauge field in between.

When it comes to implementation of the lattice gauge theories in a numerical simulation or in an experiment, the infinite Hilbert space of each gauge field has to be fit into a finite Hilbert space imposed by memory constraints of the computer or by the physical degrees of freedom of the quantum simulator. Various techniques for truncation of the infinite gauge field Hilbert space exist. However, regardless of the precise implementation, the gauge symmetry has to remain unaltered. One possibility is to consider the Quantum Link Model (QLM) representation [18], where the local Hilbert space on each link is given by that of a spin-S object. In the QLM formulation of quantum electrodynamics, the electric field operator E_n on a link is replaced by the spin-Z operator eS_n^Z; the link operator $U = \exp ieA_n$, which describes the dynamical Peierls phase picked up by a fermion moving from lattice site n to $n+1$ and which raises the electric field by one unit, is replaced by $[S(S+1)]^{-1/2}S_n^+$.

For our purpose, we consider a slight modification of the QLM, first considered in [19] and used in various works ever since, most recently in [20, 21], presented under the name truncated Schwinger model (TSM). In the TSM, we have the same Hilbert space as in the QLM; however, the link operator is replaced by the operator $\tilde{S}^+$, whose matrix elements are given by $[\tilde{S}^+]_{i,j} := \delta_{j,i+1}$. By its definition it is evident that the operator $\tilde{S}^+$ looks like the bulk of the unitary link operator U, but with a hard cutoff.

Specializing to two flavours, the Hamiltonian of the TSM including the $\theta-$angle reads

$$\begin{aligned} H_{\text{TSM}} =& \frac{e^2 a}{2}\sum_n (S_n^z)^2 + \frac{e^2 a\theta}{2\pi}\sum_n S_n^z + \frac{e^2 a}{8\pi^2}\theta^2 \\ &+ \sum_{n,p}(-1)^{n+p-1} m_p \phi^\dagger_{n,p}\phi_{n,p} \\ &- \frac{i}{2a}\sum_{n,p}(f_{n,p}\phi^\dagger_{n,p}\tilde{S}^+_n\phi_{n+1,p} - \text{h.c.})\,, \end{aligned} \tag{7}$$

where for flavor-twisted boundary conditions we use $f_{n,p} = -1$, if $n = L$ and $p = 2$ and $+1$ otherwise. Here, we chose to stagger the two flavours in opposite ways. Namely, the first flavour's particles (anti-particles) live on even (odd) sites, and opposite for the second flavour. This trick allows us to preserve a discrete chiral symmetry on the lattice, present in the continuum Schwinger model [22, 23].

The operator $\tilde{S}^+_n$ deserves a little more discussion. First of all, as mentioned above, it replaces $U_n = \exp ieA_n$, and we can no longer define a semiclassical winding of the vector potential A; we will find further below that nevertheless the fractons can clearly be revealed. Further, by construction this operator coincides with the unitary U excepting for a hard cutoff at $E_n = \pm S$. As a result, rather than $[E_n, U_m] = e\delta_{nm}U_m$ and $[U_n, U^\dagger_m] = 0$, it obeys the commutation relations

$$[S^z, \tilde{S}^\pm] = \pm\tilde{S}^\pm, \tag{8a}$$

$$[\tilde{S}^+, \tilde{S}^-] = |S\rangle\langle S| - |-S\rangle\langle -S|\,. \tag{8b}$$

Notably, the right hand side of Eq. (8b) is different from zero only in the extremal levels of each electric field. Even though the TSM does not asymptotically converge to the lattice Schwinger model as the QLM [21], but rather coincides with it for infinite spin length, one may thus speculate that the TSM captures well the low-energy properties of the (untruncated) Schwinger model, something that we indeed confirm below numerically. To quantify the deviation from the lattice Schwinger model, we introduce

$$\Delta U^2 = \sum_n \langle[\tilde{S}^+, \tilde{S}^-]^2\rangle = \sum_n \langle P^0_n + P^{2S}_n\rangle, \tag{9}$$

which essentially measures how strongly the link operator fails to be unitary.

In the following, we will present compelling evidence for the presence of fractons in the TSM already at small spin truncations ($S \geq 2$). Furthermore, we will show that for spin lengths $S \geq 3$, the chiral condensate in the ground state of the TSM is essentially the same as the one in the continnum Schwinger model. We also show that the size of the quantity in Eq. (9) is correlated with quantitatively accurate results for the chiral condensate with respect to the semi-classical continuum prediction.

2.3 Numerical methods

To perform numerical simulations we have developed codes based on two techniques: exact diagonalization (ED) using the QuSpin package in Python, employed for system sizes up to $L = (4 \text{ sites} + 4 \text{ links})$, with a spin $1/2$ on each site and up to spin 5 on each link; and tensor network (TN) calculations using ITensors in Julia, with system sizes up to $L = (20 \text{ sites} + 20 \text{ links})$ and similar spin sizes as for ED. The maximal bond dimension used in the MPS representation of the variational state is $\chi_{max} = 500$, which we found sufficient for obtaining converged results. Slightly larger system sizes are in principle possible for the numerical codes, but we found the results for the considered physical observables to be compatible with the analytical model within the system sizes treated in the results. Both methods are sign-problem free and work in an unbiased way also at strong coupling.

For the TN simulations, we have developed codes based on an MPS implementation of the DMRG algorithm for approximating ground states of quantum many-body models. For this purpose, we use the Julia package ITensors. In order to save computational resources, we use a unitarily equivalent formulation of the two-flavour TSM. The derivation of this Hamiltonian will be exposed in a scientific publication, together with several non-trivial extensions. In $1 + 1d$, it allows for reducing the degrees of freedom by one per lattice site, a convenient resource economy for our numerics. For the numerical calculations shown below, we implement the dimensionless version [24] of the Hamiltonian of Eq. (7): $H \to H/e^2a$.

These codes will become highly valuable also during the further continuation of the project, in particular to predict and benchmark quantum-simulation experiments of lattice gauge theories.

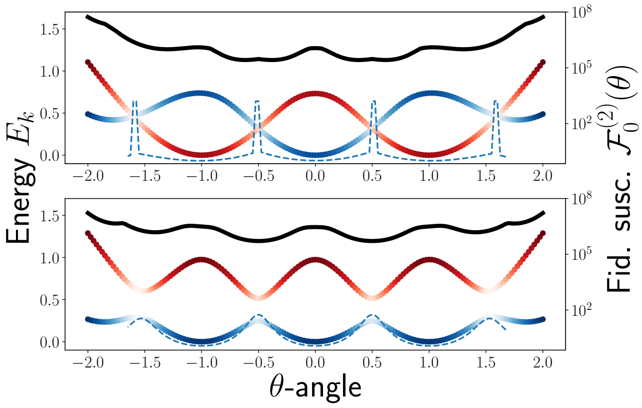

FIG. 1. **Integer vs. fractional θ-dependence in the multi-flavour TSM:** The lowest three energy levels of the TSM Hamiltonian in case of twisted (upper panel) and periodic (lower panel) boundary conditions as a function of the $\theta-$angle. In the former case, at $\theta = \pm\pi$, the two lowest lying states cross and the fidelity susceptibility (blue dotted line) exhibits a strong peak. This indicates a rapid change in the properties of the ground state, suggesting that the periodicity of the ground state is 4π. In contrast, in case of periodic boundary conditions avoided crossing occurs at $\theta = \pm\pi$ with only a broad feature in the fidelity susceptibility, rendering the period of each energy level 2π.

2.4 Results

In this section, we present our main results on the fracton excitations in the multi-flavor Schwinger model, in particular how they can be made visible in small, strongly-correlated lattice models amenable for quantum simulation.

2.4.1 Fractional ground-state behavior from exact diagionalization

To obtain a direct evidence for the existence of the fractons in the TSM, we study the lowest energy states as a function of the topological theta angle. For small non-zero fermionic mass, $m_p = m \neq 0$, continuum path-integral calculations predict the N lowest energy levels of the N-flavour Schwinger model to oscillate as a function of the theta angle as [25]

$$E_k(\theta) = -2m \exp\left(-\frac{\pi}{N\mu eL}\right) \cos\left(\frac{\theta + 2\pi k}{N}\right), \tag{10}$$

where $k \in \{0, \cdots, N-1\}$. The fracton configurations become manifest through the 2π periodicity of the fraction θ/N, rather than only θ as one is used to from the single-flavor Schwinger model. For example, for $N = 2$, there are exact level crossings at $\theta = \pm\pi$, where the ground and first excited state switch roles, resulting in an enlarged θ periodicity of 4π. This fractional theta-dependence is the precise signature we are looking for.

In the upper panel of Fig. 1, the three lowest energies of the TSM with $S = 2$ are plotted as a function of the topological theta-angle. We observe a clear gap closing at the points $\theta = \pm\pi$. To further corroborate this result, we compute the fidelity susceptibility [26–28] (see Appendix A for technical details) of the ground state. The delta-like peak shows that at $\theta = \pm\pi$ the properties of the ground state change rapidly, indicating an actual crossing. In accordance with Eq. (10), this implies a fractional theta-dependence of the ground state, resulting in the observed periodicity of $\theta = 4\pi$. In contrast, for periodic boundary conditions, the gap remains non-zero even at $\theta = \pm\pi$, as shown in the lower panel of Fig. 1. Accordingly, the fidelity susceptibility shows only a broad peak at these points, indicating no drastic property change in the ground state, in accordance with an integer theta dependence, giving the periodicity of $\theta = 2\pi$.

Remarkably, the fracton signature derived from continuum calculations in the small-m limit persists in a wide range of values of the different parameters in the Hamiltonian, as well as already for very small lattice sizes (in the figure, $S = 2$ and $L = (4$ sites $+ 4$ links$)$).

2.4.2 Tensor network calculation of the chiral condensate

We obtain further evidence for the presence of fracton configurations in the lattice TSM by investigating the chiral condensate. On the lattice with staggered fermions, the chiral condensate becomes

$$\langle\bar{\psi}\psi\rangle = \frac{1}{L}\sum_n (-1)^n \hat{\phi}_n^\dagger \hat{\phi}_n, \tag{11}$$

where we suppressed the flavour index. Figure 2 displays the main results of our DMRG simulations, for the range of physical volume $eL \in [0.4, 9.0]$, values for the lattice spacing $a \in [0.1, 0.5]$, and spin truncation $S = 3$. As the twisted boundary conditions break chiral symmetry, a finite volume can support a non-vanishing chiral condensate. Quite

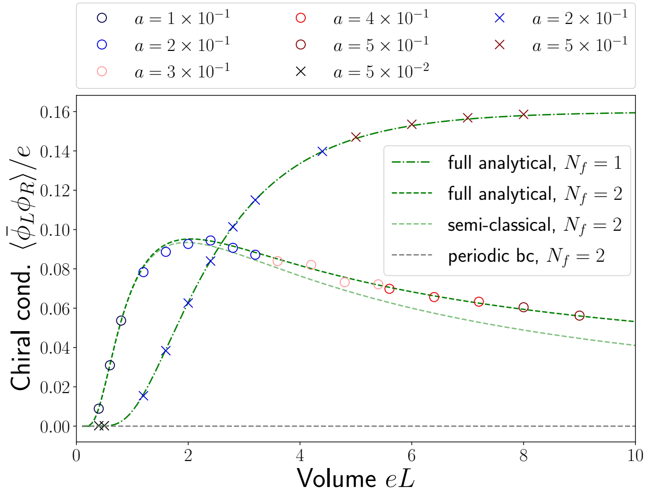

FIG. 2. **Chiral condensate as a function of the volume in the truncated Schwinger model for spin length $S = 3$:** The numerical results for the expectation value of the chiral condensate in the approximate ground state for one flavour and for two flavours with twisted boundary conditions coincide with the analytic results from the continuum Schwinger model. This accordance holds true beyond the semi-classical approximation. The results are robust w.r.t. the finite discretisation on lattice and hold already for small lattice volumes.

surprisingly, even for the coarse truncation of $S = 3$, we encounter throughout the entire range of volumes considered a quantitative agreement between the lattice calculations and the analytical predictions for the continuum Schwinger model [5]. The insignificance of lattice artifacts on the chiral condensate is quite remarkable, considering we do not take the continuum limit [24] and that lattice spacings used are as large as $a = 0.5$. In the next paragraph, we quantify this statement more precisely. Before that, we note that the same analysis can be made for the single-flavour Schwinger model. Again, the lattice results with $S = 3$ essentially coincides with the continuum prediction for lattice spacings $a \leq 0.5$. As the single-flavour Schwinger model explicitly breaks chiral symmetry, in this case the chiral condensate saturates to a finite value at $L \to \infty$. In contrast, the one for the two-flavour model with twisted boundary conditions falls off to zero at large L, highlighting the fact that the effect of boundary conditions disappears for infinite volume.

By means of Eq. (9) we can monitor finite spin truncation errors in the TSM. In FIG. 3,

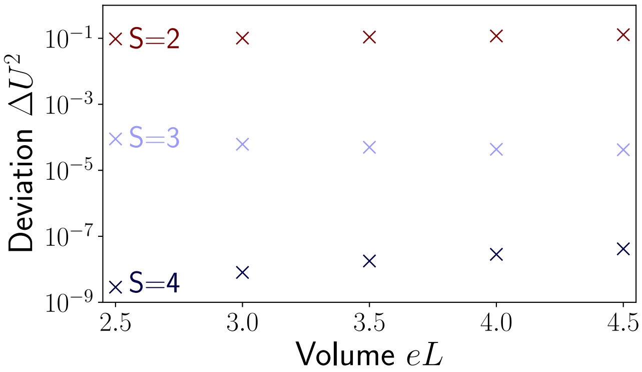

FIG. 3. **Violation of the unitarity of the link operator in the ground state of the TSM as a function of the lattice volume for different spin trunctations:** Occupation of the highest energetic states on each link due to finite truncation of its Hilbert space contribute to deviations from the untruncated Schwinger model. Already for small spin lengths $S = 3$, this deviation falls below a permille, whereas the suppression with the spin length is exponential.

we show the quantity ΔU^2 in a range of lattice volumes for spin lengths $S = 2, 3,$ and 4. We observe that already for spin length $S = 3$ in the range of investigated volumes, the occupation of the most energetic levels of the gauge fields is below a permille. Furthermore, the spin length truncation very prominently affects the violation of the commutation relation (Eq. (9)); the suppression of the error is exponential in the spin length. The quantity ΔU^2 gives a measure on the truncation error w.r.t. the untruncated Schwinger model in any dimension and with arbitrary number of flavours.

2.5 Quantum simulation through a variational protocol and number of required qudits

The physics discussed above can be probed in near-term quantum simulators, which can provide a direct demonstration of fractons in an experimental setting. A promising route is via adapting the VQE protocol previously developed at UIBK [30] to the NeQST qudit quantum processor [31], to target the ground state of the multi-flavour TSM. This model can be mapped onto a local spin Hamiltonian as in a recent proposal

Number of charges	$N_f = 1$	$N_f = 2$	$N_f = 3$	$N_f = 4$
0	$\|0\rangle$	$\|00\rangle$	$\|000\rangle$	$\|0000\rangle$
1	$\|1\rangle$	$\|10\rangle$, $\|01\rangle$	$\|100\rangle$, $\|010\rangle$, $\|001\rangle$	$\|1000\rangle$, $\|0100\rangle$, $\|0010\rangle$, $\|0001\rangle$
2	x	$\|11\rangle$	$\|110\rangle$, $\|101\rangle$, $\|011\rangle$	$\|1100\rangle$, $\|1010\rangle$, $\|1001\rangle$, $\|0110\rangle$, $\|0101\rangle$, $\|0011\rangle$
3	x	x	$\|111\rangle$	$\|1110\rangle$, $\|1101\rangle$, $\|1011\rangle$, $\|0111\rangle$
4	x	x	x	$\|1111\rangle$

TABLE I. If the matter is integrated out, as in Ref. [29], the electric field contains the information about how many charges q occupy a given vertex (first column). For a given number of flavours N_f, there are $\binom{N_f}{q}$ possibilities of fermion occupations to obtain a charge of q.

developed by the NeQST consortium [29]. As it was shown in that work for the single-flavor lattice Schwinger model, already shallow variational circuits composed of native operations on the trapped-ion qudit platform (single qudit rotations plus entangling Mølmer–Sørensen gates) provide a high-fidelity parametrization of the ground state.

While the precise scaling of required variational layers cannot be predicted analytically, we have found that already few layers of entangling gates are typically sufficient to prepare ground states with high fidelity [29]. Notably, in the trapped-ion quantum simulator, the closed boundary conditions necessary for the chiral condensation can be easily encoded in the variational ansatz due to the all-to-all connectivity.

The relevant physical observables can be easily extracted from the variational wave function. In particular, the chiral condensate can be measured in a wide range of physical volumes and for various couplings, which just correspond to a change of target parameters in the variational circuit. Further, since the TSM Hamiltonian can be mapped onto a local spin Hamiltonian [29], the number of measurements for accurate estimation of the energy will scale only linearly with system size.

As the above numerical analysis illustrates, already system sizes as small as 4 matter sites and 4 gauge links are sufficient for detecting chiral condensation due to fractons. For $N = 2$, the fermionic sites can be implemented in 4 qubits (for keeping track of the flavor index of the matter) plus 4 qudits to represent the gauge links. This corresponds to chains of 8 ions, fitting perfectly into already existing qudit devices [31].

Larger N can be realized in the same vein by integrating out the matter via Gauss's law. Due to this local conservation law, the electric fields account for the total charge at each vertex. Qudits placed on the matter sites can then be used for keeping track of the fermion flavor configuration. E.g., in the limit of one fermion per site, one requires $\binom{N}{1}$ levels, such that the NeQST trapped-ion processor can naturally implement up to $N = 7$. In the worst case, when half of the flavours are present (i.e., a charge of $N/2$ at a specific matter site), one needs to identify which flavor configuration out of $\binom{N}{N/2}$ is realized. Table 2.5 indicates the possible configurations of each lattice site in the form of a Fock state for different total charge and for N_f flavours in the model. For $N_f = 4$, the number of possible configurations is 6, so that 4 flavours fit into the 7 levels available in the NeQST trapped-ion processor.

Moreover, since already very coarse truncations of the electric field are sufficient ($S = 2, 3$), the dimensionality of the qudits can be as small as $d = 5$ for detecting fractional $\theta-$oscillations in the energy levels and as small as $d = 7$ for quantitative agreement with continuum results. Both fit into the available level structure of the trapped-ion species used in the NeQST consortium, enabling the implementation of each gauge link in a single ion qudit.

Thus, up to $N = 4$ (or 7) and $S = 3$, the scaling of spatial resources is equal to the number of lattice sites. Larger values of N and S could be achieved by decomposing into several qudits, where the scaling of spatial resources still remains linear.

3 Conclusions and Outlook

In this deliverable report, we have analyzed fractional gauge field configurations — a version of instantons with a fractional topological charge—and how they contribute to the build-up of a chiral condensate in the Schwinger model with multiple fermionic flavours. Going beyond semi-classical approximations, we have demonstrated the presence of fractons in a strongly-correlated many-body lattice model for various system sizes and in a range of values for the mass and the coupling constant. We have identified the smallest spin truncation ($S = 3$), for which the results for the chiral condensate in the zero-mass limit agree quantitatively with the predictions from the (1+1)-d continuum QED. Qualitative agreement is achieved already at even lower truncations such as $S = 2$. Quite surprisingly, these agreements hold already for relatively small system sizes and large values of the lattice spacing, thus allowing to extract valuable information about the system without taking the continuum limit.

Further, we have provided an implementation plan bespoke for the trapped-ion platform of the UIBK partner of NeQST. Thanks to intensive theoretical and numerical analysis, we were able to identify smoking gun signatures of fracton excitations, and to evaluate the minimal resource requirement to implement. Quite surprisingly, although the key arguments for the relevance of fractons derive from semi-classical continuum analysis, they become clearly visible in small, highly truncated, and strongly-coupled lattice theories, which we have found to perfectly fit the resources available in current trapped-ion qudit setups. Based on these analyses, benchmarks, and insights, work on the experimental implementations of this model and its rich physics are ongoing.

Simultaneously, UIBK experimentally implemented an equally interesting setting of Abelian gauge theories, namely proceeding towards higher dimensions through the implementation of an Abelian gauge theory in $2 + 1$d including both matter and gauge fields [32]. This addresses an outstanding frontier of current gauge-theory quantum simulation [33]. The interactions between the consortium partners have also stimulated new protocols to mitigate errors of gauge-symmetry in experiments, based on weak measurements or on error-correcting codes [34–36].

In this deliverable report, we have restricted our analysis to low numbers of flavours coupled to the $U(1)$ gauge field. Immediate extensions could investigate large numbers of fermionic flavours—a testbed for probing phenomena like chiral phase transition in QCD. Even though we have proven signatures of gauge configurations with fractional topological charge, understanding their origin beyond semi-classical arguments remains unresolved. A future research direction could be to develop a characterization in terms of topological invariants valid for a many-body system with local gauge symmetry.

Looking further, the insights achieved and expertise developed at the levels of hardware, simulation and control software, as well as algorithm development will be of high relevance to the future activities of the NeQST project and beyond. For example, the expertise acquired on experimental realizations of lattice gauge theories will be of large benefit for the development and implementation of more complicated theories; the numerical codes to benchmark the models will be used to advance the development of a numerical simulation suite for the qudit platform; and the experience with constraints in variational algorithms will stimulate development of optimization problems.

A Fidelity susceptibility

In this appendix, we give a few details on the fidelity susceptibility of the ground state, shown FIG. 1 as a function of the $\theta-$angle. The fidelity susceptibility is defined as

$$\mathcal{F}_0^{(2)}(\theta) = \frac{\partial^2}{\partial \delta^2} |\langle \psi(\theta)|\psi(\theta+\delta)\rangle|^2|_{\delta=0}. \tag{A1}$$

This quantity is used to indicate phase transitions and rapid changes of the properties of the corresponding state. If the fidelity susceptibility exhibits a delta-like peak in a certain point, the properties of the corresponding state changes and this means that a crossing occurs—the properties of the lower-lying state to the left of the crossing point are different from those of the lower-lying state to the right. In practise, we compute the discretised version of this quantity,

$$\begin{aligned}\mathcal{F}_0^{(2)}(\theta,\delta) = \frac{1}{\delta^2}\big[&|\langle \psi(\theta)|\psi(\theta+\delta)\rangle|^2 \\ &+|\langle \psi(\theta)|\psi(\theta-\delta)\rangle|^2 - 2\big],\end{aligned} \tag{A2}$$

for a sufficiently small $\delta = 0.025$. Further decrease of δ leads to a narrowing of the peak and exploding of its amplitude in case of twisted boundary conditions and no significant change in case of periodic boundary conditions. The fact that the fidelity susceptibility behaves differently for tbc w.r.t. pbc means that the periodicity in θ in the former case is 4π, whereas in the later case it is 2π.

[1] M. Creutz, L. Jacobs, and C. Rebbi, Monte carlo study of abelian lattice gauge theories, Phys. Rev. D **20**, 1915 (1979).

[2] C. Gattringer and C. B. Lang, *Quantum chromodynamics on the lattice*, Vol. 788 (Springer, Berlin, 2010).

[3] F. Gross *et al.*, 50 years of quantum chromodynamics, The European Physical Journal C **83**, 1125 (2023).

[4] E. Poli, T. Bland, S. J. M. White, M. J. Mark, F. Ferlaino, S. Trabucco, and M. Mannarelli, Glitches in rotating supersolids, Phys. Rev. Lett. **131**, 223401 (2023).

[5] M. A. Shifman and A. V. Smilga, Fractons in the twisted multiflavor schwinger model, Phys. Rev. D **50**, 7659 (1994).

[6] T. V. Zache, N. Mueller, J. T. Schneider, F. Jendrzejewski, J. Berges, and P. Hauke, Dynamical topological transitions in the massive schwinger model with a θ term, Phys. Rev. Lett. **122**, 050403 (2019).

[7] V. Kasper, G. Juzeliūnas, M. Lewenstein, F. Jendrzejewski, and E. Zohar, From the jaynes–cummings model to non-abelian gauge theories: a guided tour for the quantum engineer, New Journal of Physics **22**, 103027 (2020).

[8] A. Mil, T. V. Zache, A. Hegde, A. Xia, R. P. Bhatt, M. K. Oberthaler, P. Hauke, J. Berges, and F. Jendrzejewski, A scalable realization of local u (1) gauge invariance in cold atomic mixtures, Science **367**, 1128 (2020).

[9] J. Fraxanet, A. Dauphin, M. Lewenstein, L. Barbiero, and D. González-Cuadra, Higher-order topological peierls insulator in a two-dimensional atom-cavity system, Phys. Rev. Lett. **131**, 263001 (2023).

[10] V. Kasper, D. González-Cuadra, A. Hegde, A. Xia, A. Dauphin, F. Huber, E. Tiemann, M. Lewenstein, F. Jendrzejewski, and P. Hauke, Universal quantum computation and quantum error correction with ultracold atomic mixtures, Quantum Science and Technology **7**, 015008 (2021).

[11] Y. Deller, S. Schmitt, M. Lewenstein, S. Lenk, M. Federer, F. Jendrzejewski, P. Hauke, and V. Kasper, Quantum approximate optimization algorithm for qudit systems, Physical Review A **107**, 062410 (2023).

[12] D. González-Cuadra, T. V. Zache, J. Carrasco, B. Kraus, and P. Zoller, Hardware efficient quantum simulation of non-abelian gauge theories with qudits on rydberg platforms, Phys. Rev. Lett. **129**, 160501 (2022).

[13] T. V. Zache, D. González-Cuadra, and P. Zoller, Fermion-qudit quantum processors for simulating lattice gauge theories with matter, Quantum **7**, 1140 (2023).

[14] L. Funcke, T. Hartung, K. Jansen, S. Kühn, M.-O. Pleinert, S. Schuster, and J. von Zanthier, Exploring the phase structure of the multi-flavor schwinger model with quantum computing, in *PoS LATTICE2022 020.* (2023).

[15] M. C. Bañuls, K. Cichy, J. I. Cirac, K. Jansen, S. Kühn, and H. Saito, The multi-flavor schwinger model with chemical potential - overcoming the sign problem with matrix product states, in *PoS LATTICE2016 316.* (2016).

[16] S. R. Coleman, There are no Goldstone bosons in two-dimensions, Commun. Math. Phys. **31**, 259 (1973).

[17] J. Kogut and L. Susskind, Hamiltonian formulation of Wilson's lattice gauge theories, Phys. Rev. D **11**, 395 (1975).

[18] S. Chandrasekharan and U.-J. Wiese, Quantum link models: A discrete approach to gauge theories, Nucl. Phys. B **492**, 455 (1997).

[19] E. Zohar, J. I. Cirac, and B. Reznik, Simulating compact quantum electrodynamics with ultracold atoms: Probing confinement and nonperturbative effects, Phys. Rev. Lett. **109**, 125302 (2012).

[20] J.-Y. Desaules, A. Hudomal, D. Banerjee, A. Sen, Z. Papić, and J. C. Halimeh, Prominent quantum many-body scars in a truncated schwinger model, Phys. Rev. B **107**, 205112 (2023).

[21] J.-Y. Desaules, E. J. Gustafson, A. C. Li, Z. Papić, and J. C. Halimeh, Robust finite-temperature many-body scarring on a quantum computer, arXiv preprint arXiv:2309.11543 (2023).

[22] F. Berruto, G. Grignani, G. W. Semenoff, and P. Sodano, Spectrum of the two-flavor schwinger model from the heisenberg spin chain, Phys. Rev. D **59**, 034504 (1999).

[23] R. Dempsey, I. R. Klebanov, S. S. Pufu, and B. Zan, Discrete chiral symmetry and mass shift in the lattice hamiltonian approach to the schwinger model, Phys. Rev. Res. **4**, 043133 (2022).

[24] M. C. Bañuls, K. Cichy, K. Jansen, and H. Saito, Chiral condensate in the schwinger model with matrix product operators, Phys. Rev. D **93**, 094512 (2016).

[25] T. Misumi, Y. Tanizaki, and M. Ünsal, Fractional θ angle,'t hooft anomaly, and quantum instantons in charge-q multi-flavor schwinger model, Journal of High Energy Physics **2019**, 1 (2019).

[26] S.-J. Gu, Fidelity approach to quantum phase transitions, International Journal of Modern Physics B **24**, 4371 (2010).

[27] P. Hauke, F. M. Cucchietti, A. Müller-Hermes, M.-C. Bañuls, J. I. Cirac, and M. Lewenstein, Complete devil's staircase and crystal–superfluid transitions in a dipolar xxz spin chain: a trapped ion quantum simulation, New Journal of Physics **12**, 113037 (2010).

[28] L. Wang, Y.-H. Liu, J. Imriška, P. N. Ma, and M. Troyer, Fidelity susceptibility made simple: A unified quantum monte carlo approach, Phys. Rev. X **5**, 031007 (2015).

[29] P. P. Popov, M. Meth, M. Lewestein, P. Hauke, M. Ringbauer, E. Zohar, and V. Kasper, Variational quantum simulation of u(1) lattice gauge theories with qudit systems, Phys. Rev. Res. **6**, 013202 (2024).

[30] C. Kokail, C. Maier, R. van Bijnen, T. Brydges, M. K. Joshi, P. Jurcevic, C. A. Muschik, P. Silvi, R. Blatt, C. F. Roos, and P. Zoller, Self-verifying variational quantum simulation of lattice models, Nature **569**, 355 (2019).

[31] M. Ringbauer, M. Meth, L. Postler, R. Stricker, R. Blatt, P. Schindler, and T. Monz, A universal qudit quantum processor with trapped ions, Nature Physics **18**, 1053 (2022).

[32] M. Meth, J. F. Haase, J. Zhang, C. Edmunds, L. Postler, A. Steiner, A. J. Jena, L. Dellantonio, R. Blatt, P. Zoller, *et al.*, Simulating 2d lattice gauge theories on a qudit quantum computer, arXiv preprint arXiv:2310.12110 (2023).

[33] E. Zohar, Quantum simulation of lattice gauge theories in more than one space dimension—requirements, challenges and methods, Philosophical Transactions of the Royal Society A **380**, 20210069 (2022).

[34] M. M. Wauters, E. Ballini, A. Biella, and P. J. Hauke, Measurement-induced error protection schemes in lattice gauge theories, in preparation.

[35] E. Ballini, M. M. Wauters, E. Tirritto, and P. J. Hauke, Gauge protection in non-abelian lgt by dynamical post-selection, in preparation.

[36] L. Spagnoli and A. Roggero, In preparation.